



Auto-Tuned Particle Swarm with perturbed velocities - Optimized CLMF Algorithm for DVR based Power Quality Improvement

Tummala Kranti Kiran^{1*}, Balakrishnan Rajagopal¹, Yerramilli Butchi Raju²

¹Department of Electrical Engineering at Annamalai University, Annamalai nagar, Tamil Nadu, India.

krantikiran82@gmail.com, ba_raj7278@rediffmail.com

²Department of Electrical Engineering at Sir C R Reddy College of Engineering, Eluru, Andhra Pradesh, India.

butchiraju.y@gmail.com

*Correspondence: krantikiran82@gmail.com

Abstract

Problems pertaining to power quality, like voltage sags and swells as well as harmonics, have the potential to impact the reliability of contemporary power systems. An innovative approach that integrates the Composite Least Mean Fourth (CLMF) algorithm with meta-heuristic algorithms like PSO, DE, PSODE and a hybridization Auto-Tuned PSO and DE (APSODE)—to enhance the performance of a Dynamic Voltage Restorer (DVR) is presented in this study. The CLMF algorithm is used mostly to mitigate voltage distortions, while the meta-heuristic algorithms are employed primarily to optimize the DVR's control parameters for improved operation over different power quality conditions. Extensive simulations, conducted in the MATLAB environment, validate the proposed method, showing a substantial improvement in voltage restoration, reduced Total Harmonic Distortion (THD), and faster dynamic response. The findings of the study highlight the effectiveness of combining CLMF with PSO, DE, PSODE and APSODE in addressing power quality issues, offering improved performance and higher adaptability to changing conditions of power system. The proposed APSODE algorithm introduces auto-tuned acceleration coefficients and hybrid velocity mutation mechanisms, offering real-time adaptability and improved convergence over traditional methods, thereby ensuring strong voltage compensation under dynamic power quality conditions.

Keywords: Dynamic Voltage Restorer, CLMF Algorithm, PSODE, APSODE, Power Quality.

Received: June 10th, 2025 / Revised: September 10th, 2025 / Accepted: September 25th, 2025 /Online: October 3rd, 2025

I. INTRODUCTION

In today's world, electricity is essential to every aspect of our lives, from powering homes to performing critical industrial operations. However, power quality can often be compromised due to various disturbances like voltage fluctuations, harmonic distortions, and sudden voltage dips. These issues can result in operational inefficiencies, equipment failures, and even significant financial losses. As industries and households rely mostly on sensitive electronic equipment, ensuring high power quality has become a top priority [1]. Amongst different power quality issues, voltage sags are mainly problematic. They affect industries, hospitals, and communication networks, where even a small drop in voltage can lead to severe consequences such as mal- functioning of medical equipment in emergencies, stalled manufacturing process, or disrupted communication [2].

Research shows that voltage sags contribute greatly to higher operational costs, making it critical to develop effective

techniques for mitigating them in time. Dynamic Voltage Restorers (DVRs) have proven to be an effective solution to voltage disturbances. These devices detect voltage fluctuations and restore voltage at its nominal level efficiently in real-time. However, achieving optimal performance of DVR requires the use of advanced control strategies that can quickly adapt to these disturbances and maintain power supply and also quality [3]. Voltage issues such as sags, swells, and harmonics can cause significant problems, ranging from damaged equipment to operational inefficiencies and increased costs [4], [5]. Conventional methods like Instantaneous Reactive Power Theory (IRPT) and Synchronous Reference Frame Theory (SRFT) [6] are commonly used to control voltage. While they are effective, these methods often rely on complex mathematical models and phase-locked loops (PLLs), which can lead to slower response and reduced adaptability in highly dynamic power systems.

Adaptive filtering techniques, such as the Least Mean Square (LMS) algorithm, have also been explored for real-time voltage correction. However, LMS struggles in noisy environments and can have slower convergence in transient conditions. The introduction of the Least Mean Fourth (LMF) algorithm improved stability and reduced noise, but challenges like slow response and steady-state errors in dynamic power grids still exist [7]. The Composite Least Mean Fourth (CLMF) algorithm is an advanced adaptive filtering technique that has shown greater potential in mitigating voltage disturbances. In a way to improve DVR performance, this paper proposes a fresh approach which fuses the CLMF algorithm with PSO, DE, a hybrid PSODE and APSODE algorithms in changing power conditions [8], [9], [10].

Artificial intelligence (AI) has started making an impact on DVR systems. Techniques like neural networks, fuzzy logic, etc. [11] are employed to optimize DVR's performance, leading to better voltage stabilization, reduced operational costs, and more adaptable and adjustable power systems [12]. The integration of machine learning and reinforcement learning has advanced DVR's capabilities, enabling real-time voltage compensation and adaptive control in dynamic grid environments [13]. Despite advancement in technology, the performance of AI-based systems often depends on the correct tuning of parameters, which is typically done heuristically [14] [15]. Particle Swarm Optimization (PSO), motivated by the deeds of birds individually and collectively, offers a systematic and efficient way to optimize the parameters. This paper combines PSO with the CLMF algorithm to optimize DVR's performance, improving voltage restoration in real-time [16]. The hybrid PSO-CLMF approach fine-tunes the control parameters of DVR system that ensures quickly adaptable to voltage disturbances. The CLMF algorithm enables rapid tracking of voltage changes and minimizes steady-state errors, while the PSO [17]-[21], DE [22]-[23] ensure that the system's parameters are dynamically optimized for the best performance. Further, the PSO and DE are combined to have a dual advantage of PSO and DE algorithms [24]-[25]. This approach maintains balance amongst accuracy, response time, and computational efficiency that are not seen properly in traditional DVR control methods.

A. Research Gap and Contributions

Although several optimization-based DVR control strategies exist (PSO, DE, hybrid PSODE), limitations remain. PSO suffers from premature convergence, DE exhibits slower exploitation ability, and hybrid PSODE does not adaptively adjust acceleration coefficients. Moreover, most DVR works have not benchmarked performance against IEEE Std. 519 [28] harmonic limits or real-time feasibility. To address these gaps, this paper makes the following contributions:

- APSODE Algorithm – introduces auto-tuned acceleration coefficients and hybrid velocity mutation, improving convergence speed and global search ability.
- CLMF-APSODE DVR Control – enhances voltage sag/swell and harmonic compensation compared to conventional PI, PSO, DE, and PSODE-tuned DVRs.
- Performance Validation – comprehensive simulation-based validation with statistical analysis, convergence

studies, and comparative benchmarks against AI-based DVR techniques.

- Real-Time Feasibility – run-time analysis indicates the feasibility for implementation of Digital Signal Processor (DSP) and Machine Learning (ML) classifiers for iterative large and small dataset adaptability, making APSODE, a practical tool for real-world deployment [29], [30].

Unlike conventional methods, which rely on static parameter settings, this PSO-optimized CLMF system with perturbed velocities (APSODE) [26]-[27] can adapt to changing power conditions, improving robustness of voltage compensation, etc. By leveraging swarm intelligence, the system can rapidly adjust to grid changes and supply high-quality power to consumers with minimal computational cost. Simulations conducted in the MATLAB environment validate the effectiveness of this hybrid approach which demonstrates improvements in voltage compensation, reduced Total Harmonic Distortion (THD), and faster dynamic response compared to traditional methods.

II. RELATED WORK

The preliminary work for the study relates to the working mechanism of the DVR in the utility system, control system of DVR, the CLMF control algorithm for DVR system and the methodology for selecting the DC bus voltage and the approach for designing filtering system. These are presented below:

A. Working Mechanism

DVR which is a series-connected solid-state device is primarily responsible for injecting the necessary compensating voltage and abnormal regulation of voltage at load side. This compensates active/reactive power in the utility system and improves working of DVR. Figure 1 (a) illustrates DVR's configuration, whereas its equivalent circuit diagram is shown in Figure 1(b). The mathematical formula is given below:

$$V_{DVR} = V_L + Z_S I_L + V_S \quad (1)$$

where, V_L represents required voltage at the load side, V_S denotes voltage under fault conditions, I_L is the current drawn by the load, Z_S indicates the load impedance.

The expression for the load current I_L is mentioned below:

$$I_L = \frac{P_L + jQ_L}{V_L} \quad (2)$$

Where, P_L and Q_L represent active and reactive power supplied to load respectively.

With reference to load voltage, the DVR's voltage is given by:

$$V_{DVR} \angle \alpha = V_L \angle 0 + Z_S I_L \angle (\beta - \theta) + V \angle \delta \quad (3)$$

Where, α is injection angle of DVR, β is load impedance angle, δ is faulty voltage angle and θ is the power angle from load side.

$$\theta = \tan^{-1} \frac{Q_L}{P_L} \quad (4)$$

The injection power phenomenon of the DVR in action is represented by:

$$\text{Where, } S_{DVR} = V_{DVR} I_L^* \quad (5)$$

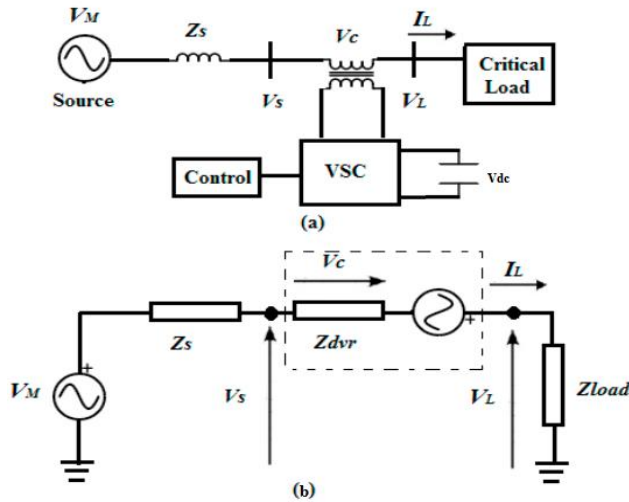


Fig. 1. (a) A diagram with DVR's configuration; (b) Equivalent circuit of the DVR

B. Control System

Figure 2 indicates the flow chart of the control scheme of DVR in which the DVR shows its functioning for compensation purpose under conditions of unexpected load and fault conditions.

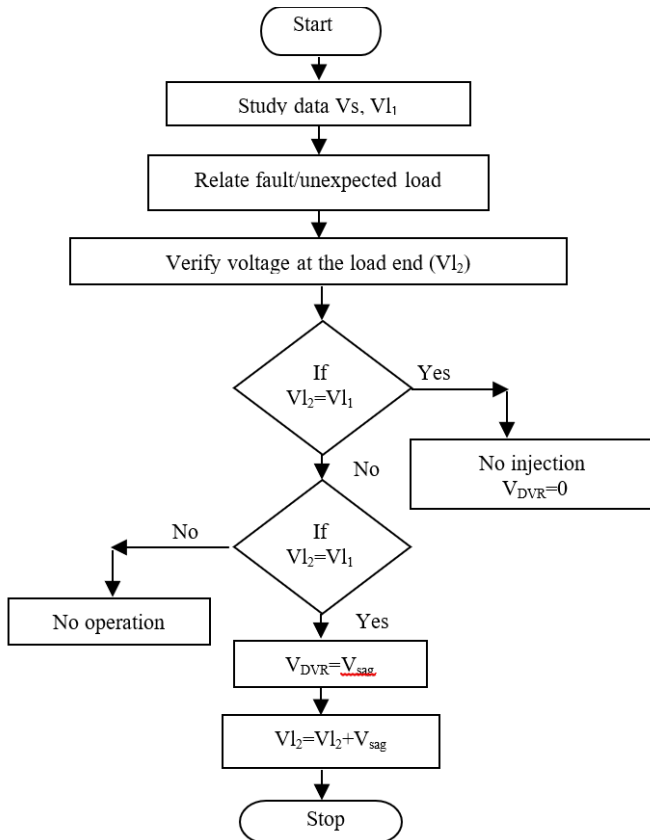


Fig. 2. Flow chart of the control scheme of DVR.

At the outset, the supply voltage (V_s) and the initial load voltage (V_{L1}) at the point of disturbance are measured, and under

normal conditions, these two values are becoming equal. When a sudden load change or fault occurs, the load voltage shifts to a new value (V_{L2}), often resulting in a voltage sag or swell. The DVR continuously monitors this change in load voltage. If V_{L2} remains equal to V_{L1} , the DVR remains inactive, indicating that no significant voltage compensation is needed—this state is referred to as standby mode. However, if V_{L2} deviates from V_{L1} , the DVR switches to active mode, injecting or absorbing voltage as needed. For sag, the DVR compensates by injecting voltage such that $V_{L1}=V_{L2}+V_{sag}$; for swell, it absorbs excess voltage, following $V_{L1}=V_{L2}-V_{swell}$. The DVR maintains this corrective action until the voltage level is restored to normalcy. The DVR's control system is crucial in determining the appropriate compensating voltage at the right time.

C. CLMF Control Algorithm

The CLMF control algorithm serves as the core control strategy of DVR, utilizing its adaptive filtering capabilities to mitigate voltage distortions efficiently. By iteratively updating the filter coefficients, the algorithm minimizes error function and ensures improved voltage stability (Figure 3).

D. System Specifications

A power supply system with a three-phase having 415V and 50Hz is a transmission utility where dynamic voltage restorer (DVR) and a non-linear load is designed in MATLAB / Simulink. The DVR system specifications are given in Table I. The methodology for selecting DC bus voltage and the approach for designing filtering system are briefed.

a) *Capacitor voltage*: The voltage across the synchronizing capacitor is given by:

$$V_{Capacitor} > 2\sqrt{2} \times V_{DVR} \quad (6)$$

b) *Voltage rating*: The peak voltage to be injected under fluctuations of voltage at the load side is applied for measuring rating of voltage. The voltage injected is approximated as:

$$V_c = \sqrt{V_s^2 - V_L^2} \quad (7)$$

c) *Ripple filter*: R_r and C_r of ripple filter series which suppresses switching frequency ripples are achieved by:

$$f_r = \frac{1}{2\pi \times R_r \times C_r} \quad (8)$$

where f_r is considered to be fifty percent of switching frequency, which ranges from 5 kHz to 20 kHz.

d) *Transformer KVA rating*: The voltage-source converter (VSC) rating of DVR which is also the injection transformer is obtained by:

$$S = \frac{3V_s \times I_s}{1000} \quad (9)$$

e) *DC bus capacitance*: The capacitance required by DVR indicates the energy needed to compensate the change in load voltage which is derived below:

$$E = \frac{1}{2} \times C_{dc}(V_{dc}^2 - V_{dc1}^2) \quad (10)$$

V_{DC} represents the nominal DC bus voltage, and V_{DC1} denotes change in DC bus voltage under abnormal conditions.

$$P \times \Delta t = \frac{1}{2} \times C_{dc}(V_{dc}^2 - V_{dc1}^2) \quad (11)$$

where, $P = 3 \times V_C \times I_S$

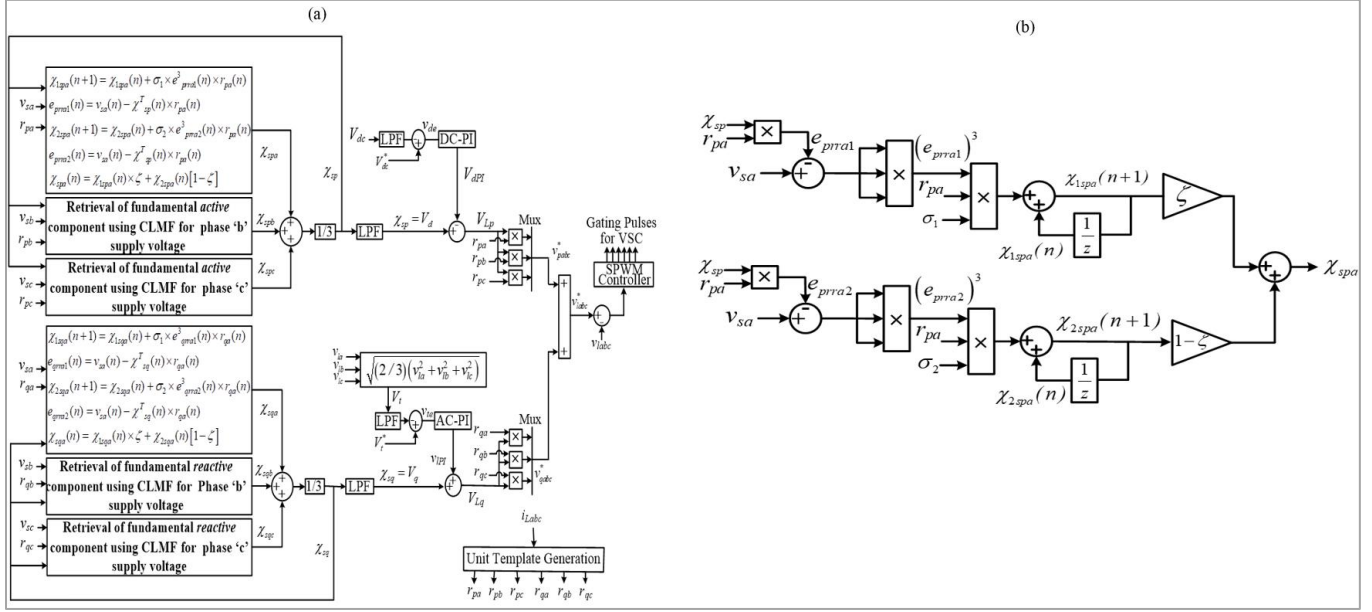


Fig. 3: (a) Composite least mean fourth (CLMF) control algorithm for DVR System; (b) CLMF phase 'a' fundamental active component extraction / retrieval.

TABLE I. DVR SYSTEM SPECIFICATIONS

| Parameter | Specification |
|------------------------------|---|
| System Voltage | 415 V (line-to-neutral), 50Hz |
| Line Impedance | $L_s=3$ mH, $R_s=0.0001 \Omega$ |
| Linear Load Resistance | $R_L=50 \Omega$ |
| Non-linear Load | R-L load of 50 Ω - 1 mH |
| Series VSI Specifications | $C_{dc}=1000 \mu F$, $C_{se}=10 \mu F$, $L_{sc}=2.1$ mH, 6 IGBTs |
| Series Injection Transformer | 1:1 ratio, 200/300V, 10 kVA |
| Series Ripple Filter | $C_f=100 \mu F$, $R_f=4.8 \Omega$ |
| DVR DC Voltage | 300V |
| PWM Switching Frequency | 10 kHz |

III. METHODOLOGY

The methodology used in the study employs both an objective function and a fitness function, aimed at minimizing the current and voltage harmonics and voltage sag/swell error.

The objective function for minimization of a multi-objective weighted case is defined as:

$$f = (w_1) \times (THD \text{ of } I_s) + (w_2) \times (THD \text{ of } V_L) + (w_3) \times (V_{ERROR}) \quad (12)$$

Where, w_1 , w_2 , w_3 are the respective weighting factors; THD of I_s is the total harmonic distortion of the source current, THD of V_L is the total harmonic distortion of the load voltage, and

V_{ERROR} denotes the deviation from the desired voltage level. This objective function serves as a foundation for the meta-heuristic algorithms used in the study to aim at enhancing DVR control and overall power quality. In this work, a weighted optimization approach is used to handle multi-dimensional objectives of power quality. The fitness function (F) is defined to minimize the combined effects of voltage sag error and current/voltage harmonic distortion. This function ensures both transient and steady-state performance improvements in the DVR system.

$$\text{Minimize, } F = f(I_{THD}) + f(V_{sag/swell}) + f(V_{THD}) \quad (13)$$

The optimal tuning parameter in this context relates to proportional (KP) and integral (KI) gains of the PI controller. The mathematical expression is represented as:

$$G_c(S) = K_p + \frac{K_i}{S} \quad (14)$$

The best values of the PI controller gains are found by the PSO, DE, PSODE and APSODE algorithms. The algorithm tracking phenomenon is shown in Figure 4.

Outputs of the controlled voltage $u(t)$ are expressed as:

$$u(t) = K_p e(t) + K_i \int_0^t e(t) dt \quad (15)$$

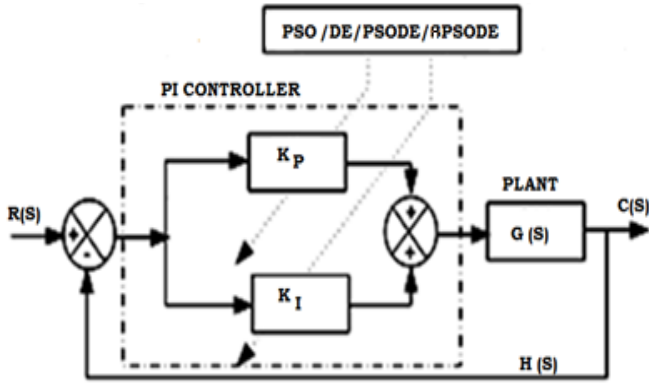


Fig.4. Example of PI Controller in action.

IV. META-HEURISTIC ALGORITHMS

Adaptive tuning of parameters is most essential to achieve the desired performance of the power system in differing operating conditions. Therefore, in this section, the meta-heuristic family of PSO, DE, PSODE and APSODE algorithms is implemented to the system network concerned that enhances the efficiency of the DVR. The structure of meta-heuristic algorithms and the related mathematical equations are mentioned hereunder:

A. Particle Swarm Optimization

The PSO algorithm is a population-based, stochastic optimization method motivated by a group of movement patterns that relate to bird flocks and fish schools. The algorithm operates by learning from environmental interactions and leveraging the knowledge to address optimization problems. Each particle is associated with a fitness value, evaluated using an objective function that is either maximized or minimized. In addition, particles are assigned velocities that influence their direction and speed of movement within the search space. The mathematical expression for position update which relates to particle over time is expressed as:

$$\begin{aligned} V_s(t+1) &= wV_s(t) + c_1r_1(p_{best} - x_s(t)) + c_2r_2(G_{best} - x_s(t)) \\ X_s(t+1) &= X_s(t) + V_s(t+1) \end{aligned} \quad (16)$$

Where: $V_i(t)$ denotes the velocity vector of the i^{th} particle over time t , $X_i(t)$ reflects position vector that relates to i^{th} particle over time t , P_{best} represents best position observed by the particle (personal best), G_{best} represents best global position given by the entire swarm, W is the inertia weight that controls the impact of both past velocity, C_1 and acceleration coefficient, C_2 called cognitive and social parameters. All are typically chosen to ensure that $C_1 + C_2 = 4$ and r_1 and r_2 , the numbers at random divided equally between 0 to 1. These are meant specifically for enhancing the stochastic behaviour of the algorithm for better optimization performance.

B. Differential Evolution (DE)

A stochastic optimization algorithm known as DE was recently introduced. Efficiency, simplicity, local search property, and speediness are the major advantages of DE. In this algorithm, two generations, i.e. old and new, of the population are considered for analysis.

Initially, mutation operation is expressed below:

$$V_i^{G+1} = V_i^G + F(V_{best}^G - V_i^G) + F(V_{r1}^G - V_{r2}^G) \quad (17)$$

F : mutation constant, $r1$, $r2$ arbitrary values, $i=1,2,...,np$ represents index of population.

This is followed by the crossover operation, in which each j^{th} component of the i^{th} offspring is generated by combining the current offspring vector V_i^G and its mutated version V_i^{G+1} . The crossover process is mathematically described as:

$$V_{ij}^{G+1} = \begin{cases} V_{ij}^{G+1}, & \text{if rand}(0,1) < CR \\ V_{ij}^G, & \text{otherwise} \end{cases} \quad (18)$$

$$\text{and } i=1,2,...,np ; j=1,2,3,...,n$$

C. Particle Swarm Optimization and Differential Evolution (PSODE)

This new hybrid algorithm has been developed by integrating the differential operator of the DE algorithm with perturbed velocity and update mechanism of PSO jointly. This combination aims at executing the strengths of both PSO and DE algorithms to enhance overall optimization performance. In this approach, the differential operator is applied to a randomly chosen particle, which does not necessarily correspond to the best-known position. This integration introduces a selection strategy within the group, effectively guiding a particle toward a new and a potentially more optimal position. Velocity update relating to PSO is adapted by incorporating the position vector strategy from DE that gives a flexible search capability.

$$\vec{\delta} = \vec{X}_k - \vec{X}_j \quad (19)$$

Updated d^{th} velocity component of i^{th} particle at target using the PSODE approach is as follows:

$$\begin{aligned} V_{id}(t+1) &= \begin{cases} \omega V_{id}(t) + \beta \delta_d + C_2 \varphi_2 (P_{gd} - X_{id}(t)) & \text{if rand}(0,1) \leq CR \\ V_{id}(t) & \text{Otherwise} \end{cases} \end{aligned} \quad (20)$$

Where, CR : accelerated crossover operation, δ_d : vector difference of d^{th} velocity component of the i^{th} target particle and β : the feature of scaling ranging in between 0 to 1.

By combining the differential operator of the DE algorithm with the velocity update of PSO algorithm, the system gains increased exploration capabilities. This update process allows the velocity to retain its previous values, especially when the differential component has little impact, ensuring the particle continues its search effectively under $CR \leq 1$.

Thus, new position \vec{T}_{ri} is calculated by adding previous position to updated particle velocity, resulting in the equation given below:

$$\vec{T}_{ri} = \vec{X}_i(t) + \vec{V}_i(t+1) \quad (21)$$

Depending on improved fitness value, particles are relocated to new position. Therefore, the objective function $f(x)$, the particle's relocation is performed as follows:

$$\vec{X}_i(t+1) = \begin{cases} \vec{T}_{ri} & \text{if } f(\vec{T}_{ri}) \leq f(\vec{X}_i(t)) \\ \vec{X}_i(t) & \text{Otherwise} \end{cases} \quad (22)$$

Hence, updated velocity makes the particle move to another location that results in a better fitness value; otherwise, it remains only at its previous position. Unlike in traditional PSO, if a particle becomes stagnant, the random mutation operator integrated into the algorithm that shifts the particle to a new position, helping it avoid local minima and go forward to identify the search space more effectively.

$$\text{if } ((\vec{X}_i(t) = \vec{X}_i(t+1) = \vec{X}_i(t+2) = \dots = \vec{X}_i(t+N))$$

then for $r = 1, 2, 3, \dots, n$

$$X_{ir}(t+N+1) = X_{min} + rand_r(0,1)(X_{max} - X_{min}) \quad (23)$$

f : fitness function, N : iterations' number allowed for tolerating constancy and X_{max} , X_{min} , the upper and lower limits of the search space.

D. Auto-tuned Particle Swarm Optimization and Differential Evolution (APSODE)

A limitation of PSO is the tendency of particles to stagnate once they have prematurely converged to a particular region of the search space. On the other side, DE faces challenges such as weak local exploitation capability and slower convergence. To overcome these issues, the PSODE algorithm incorporates differential operator into PSO velocity update, enhancing both exploration and exploitation abilities. Here, differential operator is called to the position vectors of two particles selected at random from the population-members and not to the respective best positions. A particle is moved towards a new position because new position gives more fitness value. But, auto-tuning particle swarm optimization with differentially perturbed velocity is an enhancement over PSODE algorithm. The APSODE's main objective is to apply auto-tuned acceleration coefficient to adjust the location of particles to speed up the search of the global fitness value. In this approach, the mutation operator from Differential Evolution is combined with the velocity component of PSO and created the APSODE algorithm. The steps involved in the APSODE algorithm are given below:

Step 1: Initialization

Preliminary population is generated arbitrarily and is represented as:

$$U_i^0 = U_{i,\min} + rand() \cdot (U_{i,\max} - U_{i,\min}), i = 1, \dots, N_p \quad (24)$$

rand () generates an equally divided number at random in between 0 to 1. It produces offspring arbitrarily. In this phase, both control variables and their corresponding velocities are randomly generated within the permissible bounds. Besides, initialization of fitness values will be given greater importance.

Step 2: Dynamic SIMULINK model is employed for evaluation purpose that leads to analysis and optimization.

Step 3: Execute the process and examine individual's fitness value.

Step 4: Mutation operation

Incorporate the mutation operator for velocity update stride of PSO. Two particles are chosen at random and the mutation operator is formulated below:

$$\delta_d = F (U_k - U_j), \quad i \neq j \neq k \quad (25)$$

Step 5: Crossover operation

Recombination also called crossover is a procedure that seeks to strengthen past successes by producing offspring from current parent individuals. To further expand the range of offspring at the subsequent creation, the agitated offspring $U_{ij}^{(t)}$ is produced from the current offspring $X_{ij}^{(t)}$ of by accumulation of the differentially agitated velocity to $V_i^{(t)}$. Recombination constant (CR) is employed for identifying whether newly produced offspring should be recombined. The velocity j for each parameter of the i^{th} offspring is based on the altered velocity of the individual V_i^{G+1} , and the updated velocity of the offspring which is expressed as follows:

$$V_{ij}^{G+1} = \begin{cases} \bar{\omega} V_{ij}^G + \delta_d + C_2 \varphi_2 (P_{gi} - X_{ij}^G), & \text{if } rand(0,1) < CR \\ V_{ij}^G, & \text{Otherwise} \end{cases} \quad (26)$$

$i=1, 2, \dots, N_p$; $j = 1, 2, \dots, n$; n is number of parameters, C_2 the acceleration coefficient, φ_2 is the random number (0,1), $\bar{\omega}$ the weighting factor, and δ_d is taken from eq. (26).

Thus, the recombination crossover formula is given by:

$$U_{ij}^{(t)} = \begin{cases} V_i^{(t)}, & \text{if } rand_j \leq CR \text{ or } j = j_{rand} \\ X_{ij}^{(t)}, & \text{otherwise} \end{cases} \quad (27)$$

Auto-Tuned acceleration coefficient C_2 is shown in eq. (28):

$$C_2 = (C_{2f} - C_{2i}) \frac{gen}{gen_{max}} + C_{2i} \quad (28)$$

Where C_{2i} , C_{2f} , are derived acceleration constants.

Weighting factor is expressed below:

$$w = w_{max} - \frac{(w_{max} - w_{min}) \cdot gen}{gen_{max}} \quad (29)$$

where, gen and gen_{max} denote the current generation number and also maximum generation number respectively.

A new trial position $X_i^{(t+1)}$ for the particle is then generated by making an addition to the updated velocity to its previous position $X_i^{(t)}$:

$$X_i^{(t+1)} = X_i^{(t)} + V_i^{(t+1)} \quad (30)$$

Step 6: Assessment and Assortment

The fitness of each offspring is compared with that of its parent. If the offspring demonstrates better fitness, it replaces the parent in the next generation. However, if the offspring performs worse, the parent is retained. These two scenarios are represented as follows:

$$X_i^{(t+1)} = \begin{cases} U_i^{(t)}, & \text{if } f(U_i^{(t)}) < f(X_i^{(t)}) \\ X_i^{(t)}, & \text{otherwise} \end{cases} \quad (31)$$

$$X_i^{(t+1)} = \arg \min \{f(X_i^{(t)}), f(U_i^{(t)})\} \quad (32)$$

arg min is meant argument of minimum which is used because the fitness function, $f = F$, where F relates to objective function that requires minimization.

Step 7: Repeat steps 2 to 6 up to the maximum generation quantity is reached. This algorithm evaluates fitness of each offspring for assessing its corresponding variables. An optimization process continues till the pre-defined generation numbers are arrived at successfully. The flowchart illustrating the suggested method is presented in Figure 5.

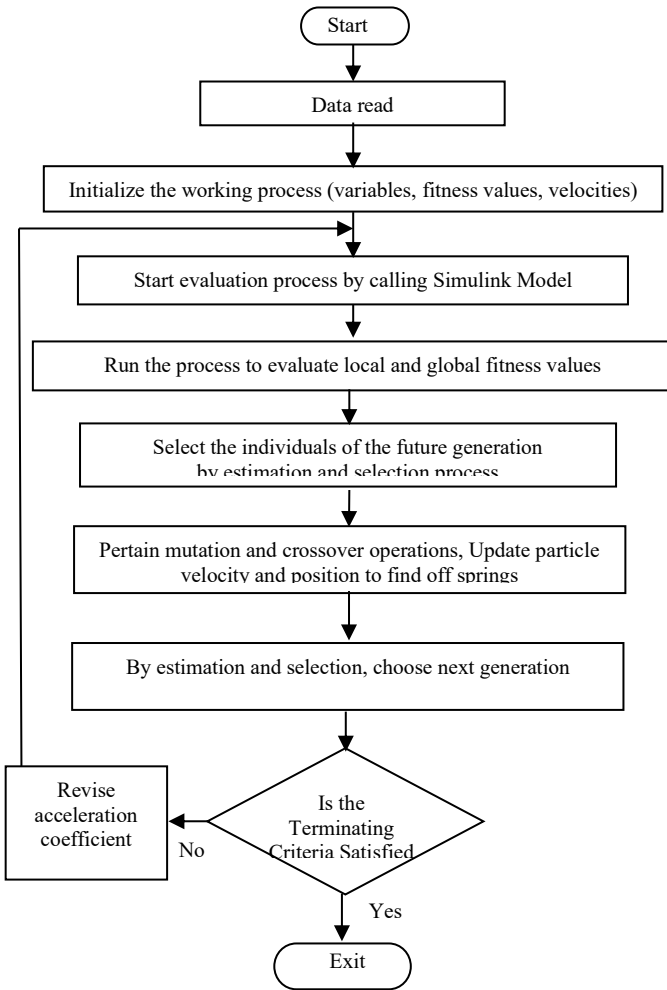


Fig. 5. Flowchart of APSODE Algorithm

V. RESULTS AND DISCUSSION

The experimentation is carried out in the MATLAB environment, focusing on the problems of power disturbances such as sag, swell, and harmonics. The corresponding system

response is depicted in Figure 6. As the nonlinear load generates current harmonics in the system, it is shown in Figure 6 (c). The DVR is inserted in the power transmission line, as shown in Figure 7. The utility power supply delivers a voltage of 415V at a frequency of 50Hz. Voltage swell conditions are simulated by introducing a sudden load change (VL2) into the system using a circuit breaker, triggered at specific time interval i.e. voltage swell is at 0.2 sec. to 0.3 sec.. According to IEEE standards, the magnitude of the voltage is increased by 10% to simulate swell conditions. During 0.2 sec. – 0.3 sec. interval, the DVR immediately reacts suitably and operates in a relevant mode to counteract the conditions of voltage swell and restore pre-disturbance conditions early. This is given in Figure 8. The proposed PSO, DE algorithms along with its hybrid models i.e. PSODE and APSODE are utilized to minimize voltage error, voltage harmonics and current harmonics. One of the key challenges of controlling voltage relates mainly to determine a suitable duty cycle. As the main objective of the study is to achieve effective voltage compensation during sag and swell conditions along with mitigating harmonic components in the source current, this section focuses on Total Harmonic Distortion (THD) analysis and the reduction of DC-link error.

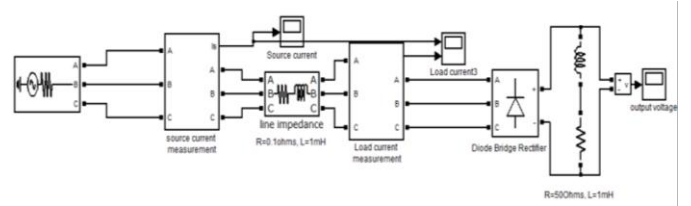


Fig. 6. (a) MATLAB/Simulink model showing a basic transmission line connected to non-linear load

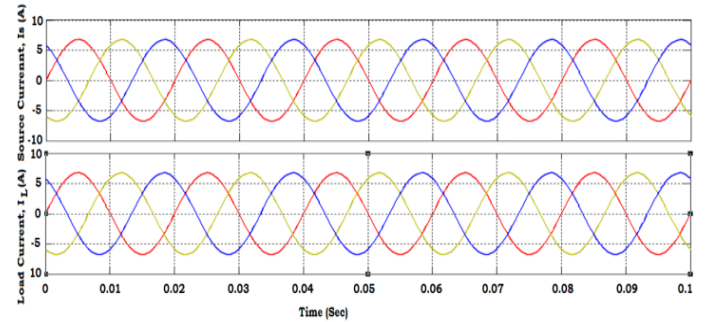


Fig. 6. (b). Source and load current waveforms of basic transmission line configuration having linear resistive load.

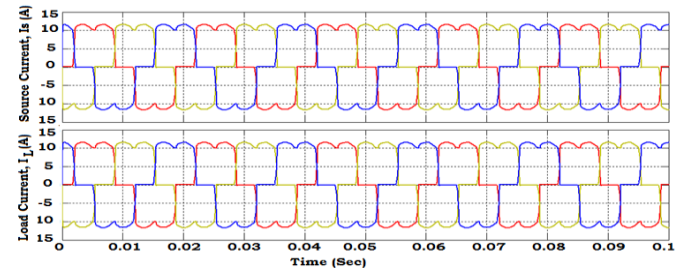


Fig. 6. (c) Source current and load current abnormalities having non-linear load.

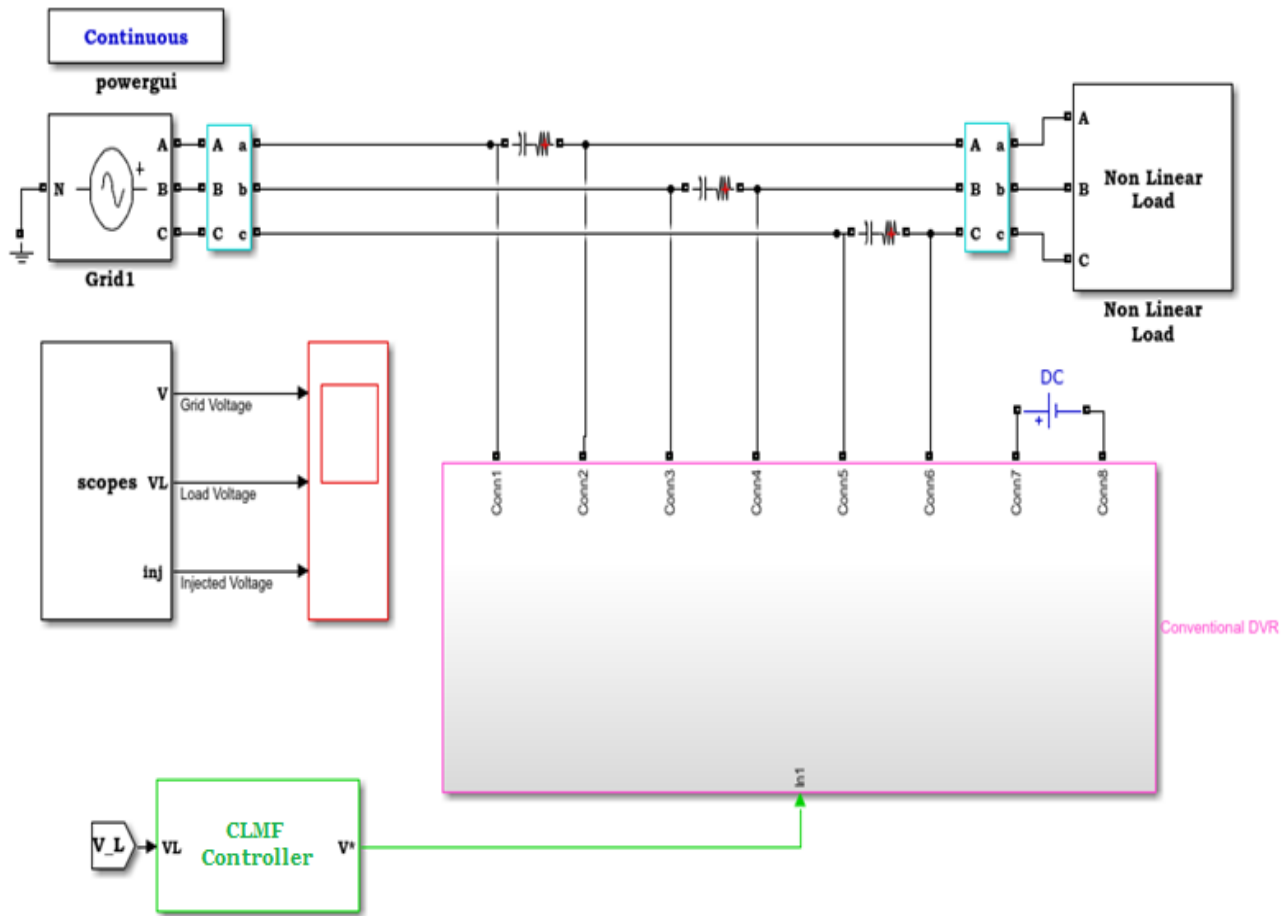


Fig. 7. MATLAB/Simulink diagram depicting integration of DVR into the utility power system.

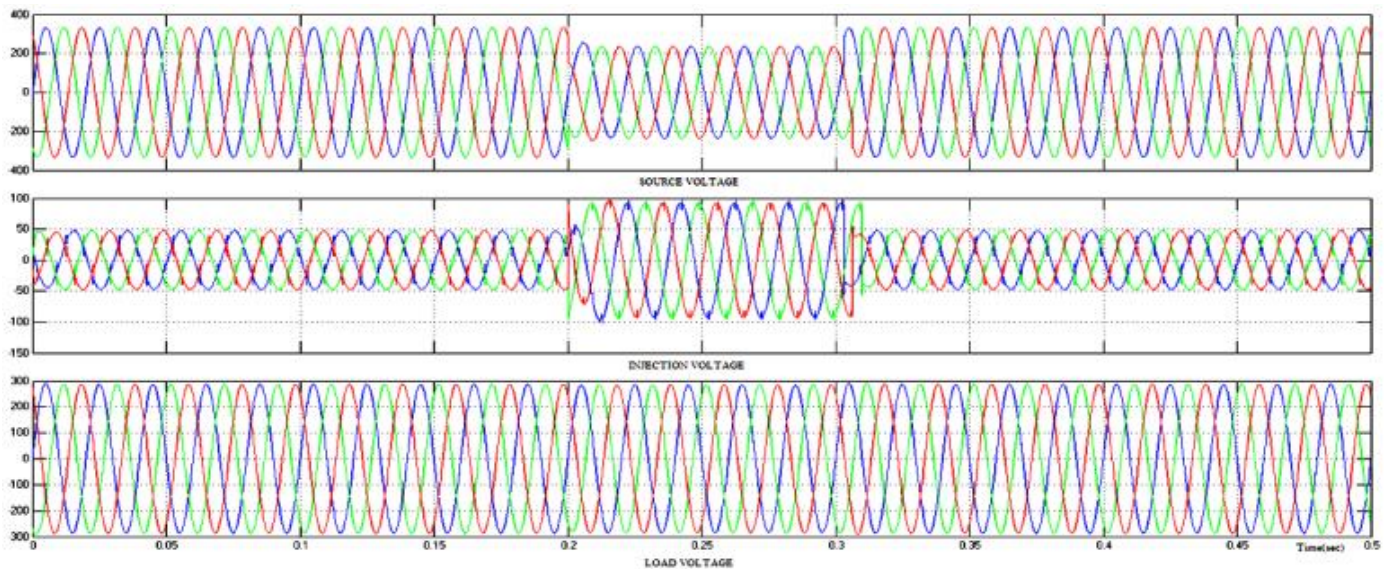


Fig. 8. Functional Performance of DVR in the power utility system

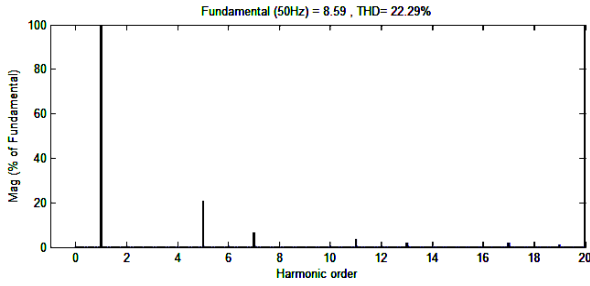


Fig. 9. THD analysis of source current with PI (trial and error) controlled DVR compensation

Without controller, the DVR exhibits the source and load currents at THD of 22.29% with Fast Fourier Transform (FFT) analysis. This is shown in Figure 9. This analysis is mainly used to convert a signal from time-domain to frequency-domain which reveals the individual frequencies, amplitudes and phases of the signal.

A. Algorithm Specifications

By implementing the proposed optimization-based control strategies, significant improvements in power quality and system stability are achieved. The specifications for implementation of the proposed algorithms are given: The population size is fixed at 10, and the iterations' number is 100. The minimum values for the K_P and K_I parameters are set to 0, with the maximum values for K_{P1} and K_{P2} being 25, and for K_{I1} and K_{I2} being 2. The maximum velocity for K_{P1} is calculated as $K_{P1max}/20$, and similarly, the maximum velocity for K_{I1} is $K_{I1max}/20$. The minimum velocities for K_{P1} and K_{I1} are the negative counterparts of their respective maximum velocities. The same calculations are applied to K_{P2} and K_{I2} also, with their velocities set similarly. For the algorithm, the acceleration constants C_1 and C_2 vary in such a way that $C_1 + C_2 = 4$. The optimal inertia (W) is constant and is obtained as follows in the PSO algorithm which varies according to the variability of iteration i.e. between 0 to 1.

$$W = \frac{\text{miniter} - \text{iter}}{\text{miniter}} \quad (33)$$

Where, *miniter*: Total number of iterations considered and *iter*: current iteration.

For DE algorithm, the CR and F are also in between 0 to 1 as per the principles of DE and evolutionary computing.

B. Performance Evaluation

This section evaluates the voltage error and the Total Harmonic Distortion (THD) of the source current and the load voltage with the Dynamic Voltage Restorer (DVR) for different meta-heuristic algorithms.

The multi-objective convergence values of fitness for sag/swell error and source current THD are minimized to 2.52% (average value after 10 runs) by using the PSO algorithm with the parameters: $K_{P1} = 3.14$, $K_{I1} = 1.60$, $K_{P2} = 6.53$, $K_{I2} = 1.10$, $C_1 = 3.0$, and $C_2 = 1.0$, adhering strictly to empirical relation $C_1 + C_2 = 4$.

TABLE II. CONVERGENCE OF CONTROL PARAMETERS (SAG/SWELL ERROR, SOURCE CURRENT THD) WITH DVR USING PSO

| C_1 | C_2 | K_{P1} | K_{I1} | K_{P2} | K_{I2} | IsTH D (%) | VsTH D (%) | VsERROR (%) |
|------------|------------|--------------|-------------|--------------|-------------|--------------|---------------|---------------|
| 3.5 | 0.5 | 11.5 | 1.1 | 15.5 | 1.0 | 25.62 | 0.2824 | 1.7089 |
| 3.0 | 1.0 | 03.14 | 1.60 | 06.53 | 1.10 | 22.67 | 0.2519 | 1.5119 |
| 2.5 | 1.5 | 12.1 | 1.5 | 06.0 | 1.9 | 24.94 | 0.2750 | 1.7505 |
| 2.0 | 2.0 | 14.1 | 1.2 | 13.2 | 1.8 | 25.59 | 0.2832 | 1.7653 |
| 1.5 | 2.5 | 02.5 | 1.3 | 09.5 | 1.7 | 25.57 | 0.2841 | 1.6891 |
| 1.0 | 3.0 | 12.3 | 1.8 | 13.5 | 1.2 | 25.86 | 0.2851 | 1.6951 |
| 0.5 | 3.5 | 15.5 | 1.1 | 11.6 | 1.3 | 25.95 | 0.2829 | 1.7029 |

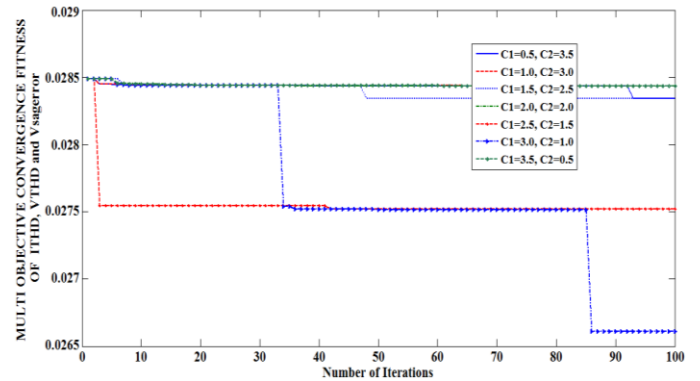


Fig. 10. Multi-objective convergence of fitness (source current THD, load voltage THD, and voltage sag error) using PSO Algorithm.

The maximum values relating to PSO-tuned K_{P1} , K_{I1} , K_{P2} , and K_{I2} are provided to the two PI controllers of DVR to evaluate the problems of power disturbances. The performance of the DVR is assessed by observing voltage before compensation, the injected or absorbed voltages, and the voltage after compensation. The multi-objective convergence is presented in Table II and Figure 10. The DE algorithm is employed differently for undertaking the optimization process. Based on literature survey and test signal verification, the best-chosen values for CR are between 0.8 and 0.9, while F ranges from 0.5 to 1.0. The series active power conditioner model is aimed at mitigating current harmonics, voltage harmonics and sag/swell error and is developed in MATLAB/Simulink environment. It is used in the DE algorithm for optimal tuning of PI controller gains. With the help of optimal tuned PI controller gains obtained, the relevant fitness convergence data are shown Table III and Figure 11.

TABLE III. CONVERGENCE OF CONTROL PARAMETERS (SAG/SWELL ERROR, SOURCE CURRENT THD) OF DVR USING DE

| C R | F | K _{P1} | K _{I1} | K _{P2} | K _{I2} | IsTH D (%) | VsTH D (%) | V _{SERRO} R (%) |
|--------|-----|-----------------|-----------------|-----------------|-----------------|---------------|---------------|-----------------------------|
| 0.9 | 0.5 | 14.5 5 | 1.4 7 | 13.1 2 | 1.8 2 | 26.00 | 0.2890 | 1.7339 |
| 0.9 | 0.6 | 16.1 1 | 1.9 7 | 16.5 5 | 1.5 7 | 24.02 | 0.2665 | 1.6019 |

| | | | | | | | | |
|-----|-----|------|-----|------|-----|-------|--------|--------|
| 0.9 | 0.7 | 13.4 | 1.5 | 18.4 | 1.5 | 24.69 | 0.2745 | 1.6469 |
| 0.9 | 0.8 | 12.1 | 1.6 | 15.1 | 1.6 | 24.65 | 0.2740 | 1.6439 |
| 0.9 | 0.9 | 10.3 | 1.0 | 11.5 | 1.3 | 26.40 | 0.2935 | 1.7609 |
| 0.9 | 1.0 | 14.5 | 1.5 | 12.3 | 1.4 | 21.81 | 0.2440 | 1.4520 |
| | | 4 | 1 | 4 | 1 | | | |
| | | 2 | 2 | 1 | 7 | | | |
| | | 5 | 9 | 5 | 5 | | | |
| | | 6 | 6 | 6 | 0 | | | |

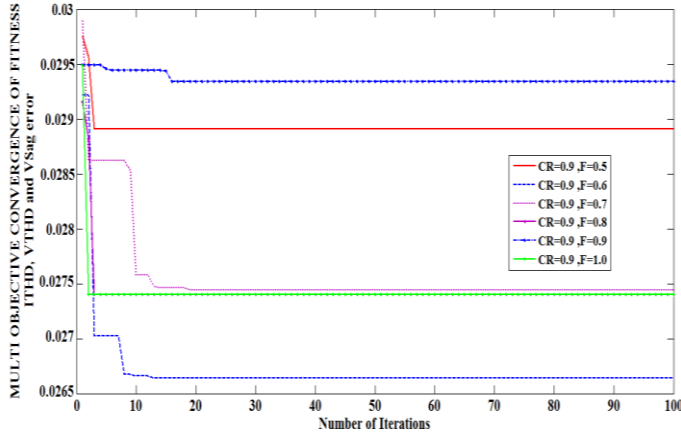


Fig. 11. Multi-objective convergence of fitness (source current THD, load voltage THD, and voltage sag error) using DE Algorithm.

The multi-objective convergence fitness value – accounting for sag/swell error and source current THD - was minimized to 2.423% (average value over 10 simulation runs) using the DE algorithm. The optimization was achieved for controller gains of $K_{P1} = 14.56$, $K_{I1} = 1.56$, $K_{P2} = 12.36$, and $K_{I2} = 1.40$, with the crossover rate (CR) set at 0.9 and the mutation factor (F) at 1.0. These values were determined after extensive evaluation of CR and F settings.

The optimal DE-tuned parameters of the DVR are applied to the PI controllers to evaluate power quality improvement. Specifically, the DVR's performance was assessed in terms of the voltage behaviour before, during and after compensation.

To rectify the inherent drawbacks of PSO and DE algorithms, a hybrid model i.e. PSODE was developed. This new method integrates the differential operator from DE into the velocity update of PSO. The PSODE algorithm improves local search capability and mitigates the stagnation issues associated with PSO. It is observed that this algorithm has not yielded same result for every run. Hence, it is followed to run a good number of times to find the average value. After running for 10 times, the fitness values at the respective adapted acceleration coefficients are presented. The fitness value is presented at $C_1=3.0$ and $C_2=1.0$ which is the respective global best. The same coefficients are also deployed in the proposed algorithms (PSODE and APSODE) when required. The acceleration coefficients in the PSODE algorithm are selected such that $C_1 + C_2 = 4$, while the mutation constant (F) is randomized within the range of 0 to 1. Based on insights from the literature, the most effective values of CR are typically between 0.8 and 0.9, and F between 0.5 and 1.0. The PSODE algorithm aims at adjusting optimally the PI controller gains, enhancing DVR's performance. The resulting convergence of the multi-objective

fitness function, following optimal tuning, is illustrated in Table IV and Fig. 12.

TABLE IV. CONVERGENCE OF CONTROL PARAMETERS OF FITNESS (VOLTAGE SAG/SWELL ERROR, SOURCE CURRENT THD) WITH DVR OF APSODE

| C_1, C_2 as 3.0 & 1.0 | | K_{P1} | K_{I1} | K_{P2} | K_{I2} | I_{sTHD} (%) | V_{sTHD} (%) | V_{sERROR} (%) |
|-------------------------|------------|---------------|-------------|------------|-------------|----------------|----------------|------------------|
| CR | F | | | | | | | |
| 0.9 | 0.5 | 16.44 | 1.64 | 15.24 | 1.37 | 24.38 | 0.2710 | 1.6259 |
| 0.9 | 0.6 | 15.45 | 1.83 | 12. | 1.40 | 26.54 | 0.2945 | 1.7699 |
| 0.9 | 0.7 | 13.51 | 1.25 | 16. | 1.54 | 26.36 | 0.2930 | 1.7579 |
| 0.9 | 0.8 | 12.50 | 1.34 | 12. | 1.74 | 22.94 | 0.2545 | 1.5299 |
| 0.9 | 0.9 | 14.688 | 1.10 | 16. | 1.36 | 21.42 | 0.2410 | 1.4430 |
| 0.9 | 1.0 | 17.64 | 1.68 | 11. | 1.97 | 22.40 | 0.2490 | 1.4939 |

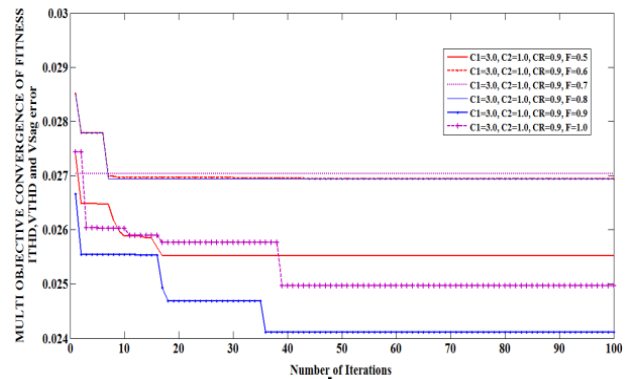


Fig. 12. Multi-objective convergence of fitness (source current THD, load voltage THD, and voltage sag error) using PSODE.

The multi-objective fitness value- accounting for sag/swell error and source current THD – was minimized to 2.398% (average over 10 simulations) using the PSODE algorithm. This optimal result was achieved with PI controller gains set to $K_{P1} = 14.68$, $K_{I1} = 1.10$, $K_{P2} = 16.42$, and $K_{I2} = 1.36$, using $C_1 = 3.0$ and $C_2 = 1.0$ in line with $C_1 + C_2 = 4$, along with a crossover rate (CR) of 0.9 and a randomized mutation factor (F). The PSODE algorithm integrates the velocity vector concept of PSO with DE operators effectively and thus enhances global search and escapes trapping from local minima. The optimized PI controller gains derived from PSODE are applied to CLMF-based DVR framework to assess the system's power quality under power disturbances and the corresponding functional performance of the DVR is evaluated. It is observed from the analysis that to enhance the rate of convergence further and to intensify the ability to update inertial weight vector and to escape local minima problem, an Auto-tuned PSODE (APSODE) is developed.

TABLE V. CONVERGENCE OF CONTROL PARAMETERS OF FITNESS (VOLTAGE SAG/SWELL ERROR, SOURCE CURRENT THD) WITH DVR OF PSODE

| C_1, C_2 as 3.0 & 1.0 | | K_{P1} | K_{I1} | K_{P2} | K_{I2} | I_{sTHD} (%) | V_{sTHD} (%) | V_{sERROR} (%) |
|----------------------------|------------|--------------|-------------|---------------|-------------|-------------------|-------------------|---------------------|
| CR | F | | | | | | | |
| 0.9 | 0.5 | 15.68 | 1.27 | 13.24 | 1.07 | 26.54 | 0.2945 | 1.76 |
| 0.9 | 0.6 | 14.62 | 1.55 | 12.25 | 1.10 | 23.39 | 0.2595 | 1.55 |
| 0.9 | 0.7 | 13.27 | 1.51 | 15.90 | 1.64 | 21.824 | 0.2420 | 1.454 |
| 0.9 | 0.8 | 12.95 | 1.68 | 14.14 | 1.74 | 23.39 | 0.2595 | 1.55 |
| 0.9 | 0.9 | 16.98 | 1.89 | 16.421 | 1.26 | 21.33 | 0.2420 | 1.44 |
| 0.9 | 1.0 | 14.25 | 1.73 | 17.14 | 1.37 | 22.85 | 0.2535 | 1.523 |

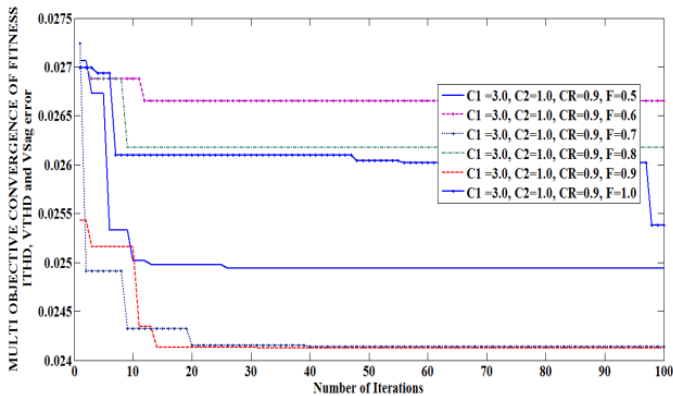


Fig. 13. Multi-objective convergence of fitness (source current THD, load voltage THD, and voltage sag error) using the APSODE Algorithm.

This study tries to reduce the problems of power disturbances such as source current harmonics, load voltage harmonics, and sags with the help of implementing a MATLAB/Simulink model in conformity with APSODE optimization algorithm. The APSODE technique is used automatically to fine-tune the PI controller gains for improved system performance. The resulting convergence patterns of the optimization process are presented in Table V and illustrated in Figure 13. After organizing ten independent runs, the algorithm successfully minimized the combined fitness value based on sag/swell error and source current THD to 2.393%. This optimal performance was obtained with controller parameters set at $K_{P1} = 16.98$, $K_{I1} = 1.89$, $K_{P2} = 16.42$, and $K_{I2} = 1.26$. The best-performing configuration used acceleration coefficients $C_1 = 3.0$ and $C_2 = 1.0$, a crossover rate $CR = 0.9$, and a randomized mutation factor F . By combining the adaptive velocity strategy of PSO with the differential mutation process of DE, the APSODE algorithm effectively avoids issues such as premature convergence, getting trapped in local optima, and slow search progress—making it a powerful tool for controller tuning in DVR-based power quality improvement.

C. Comparative Analysis

The better convergence illustrations with PSO, DE, PSODE, APSODE algorithms for their better acceleration coefficients are illustrated in Fig.14. The objective function is optimized for 100 iterations.

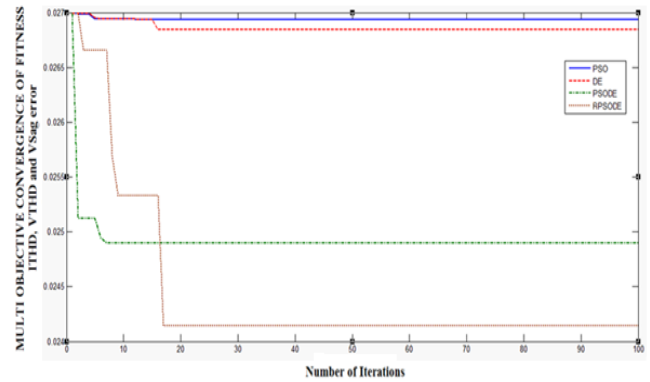


Fig. 14. Comparison of fitness convergence illustrations with PSO, DE, PSODE, APSODE algorithms

TABLE VI. PI CONTROLLER GAINS IN DVR WITH PSO, DE, PSODE, APSODE ALGORITHMS FOR THE BEST RUN

| Parameter Variable | PSO | DE | PSODE | APSODE |
|--------------------|-------|-------|--------|--------|
| K_{P1} | 03.14 | 14.56 | 14.688 | 16.98 |
| K_{I1} | 1.60 | 1.56 | 1.10 | 1.89 |
| K_{P2} | 06.53 | 12.36 | 16.421 | 16.421 |
| K_{I2} | 1.10 | 1.40 | 1.36 | 1.26 |

Table VI shows the control parameters corresponding to the best-performing run that are based on the fitness function. These are compared with different techniques which include the conventional PI controller and the evolutionary algorithms i.e. PSO, DE, PSODE, and APSODE. This comparison highlights the effectiveness of each method in tuning the PI controller gains for enhanced performance in mitigating power quality issues.

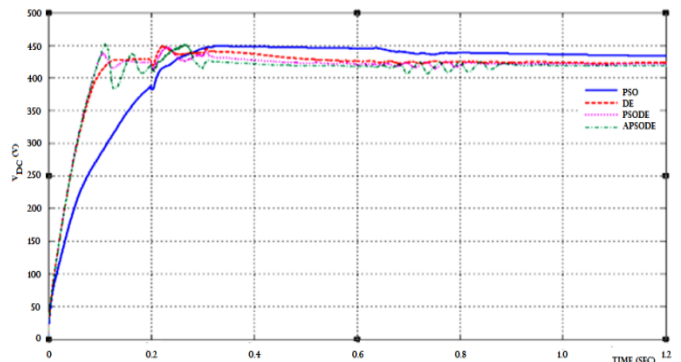


Fig. 15. Comparison of Capacitor link voltage in DVR with PSO, DE, PSODE, APSODE Algorithms

Figure 15 also indicates the response relating to DC link capacitor during sag/swell compensation which highlights specifically the performance of PI controller with PSO, DE, PSODE and APSODE algorithms.

TABLE VII. COMPARATIVE ANALYSIS OF DVR'S PERFORMANCE USING PI CONTROLLER (TRIAL AND ERROR) WITH PSO, DE, PSODE, APSODE ALGORITHMS

| Parameter Variable | IsTHD(%) | VsERROR(V) | V _{DC} (Reduced Rating) rating |
|--------------------|----------|------------|---|
| PI | 22.29 | 16.852 | 95.832 |
| PSO | 22.67 | 0.2519 | 160.79 |
| DE | 21.81 | 0.2440 | 165.80 |
| PSODE | 21.42 | 0.2410 | 169.60 |
| APSODE | 21.33 | 0.2420 | 171.56 |

Table VII and Figure 16 give performance of DVR with PI controller in PSO, DE, PSODE, APSODE algorithms after complete evaluation and study of the variation of acceleration coefficients and other parameters and are within IEEE Std 19-2022 [28] for harmonic limits for power quality. IEEE 519 sets limits for users at the Point of Common Coupling, the place where electrical system connects to the utility grid. This physical location serves as a critical interface for assessing correctly the power quality. Hence, at this point, limits on voltage harmonics are usually stricter and a total harmonic distortion (THD) of 5% is fixed rigorously. The limit for current harmonics, however, depends on how strong the systems short-circuit is. Meanwhile IEC standards, such as IEC 61000-3-2, also set rules for harmonics produced by specific equipment individually. These standards control the amount of current distortion allowed from devices that have a rated current of 16A or less, which are connected mainly to the low-voltage grid.

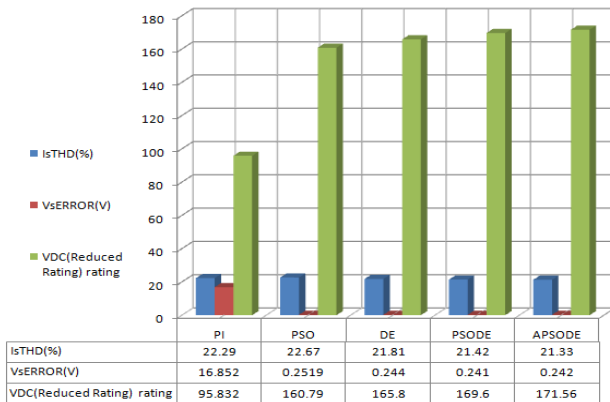


Fig. 16. Performance of DVR with PI controller in PSO, DE, PSODE, APSODE algorithms.

VI. SUPERIORITY AND REAL-TIME ADAPTABILITY

It is observed that the APSODE algorithm has the adequate mechanism to tune the acceleration coefficients automatically. In addition, the hybrid approach of this algorithm has also the capacity for real-time adaptability. It results in better convergence over other traditional algorithms of DVR control. As such, this algorithm ensures better voltage compensation

under changing power conditions in an overall perspective. Table VIII has given the comparative results of all the algorithms to prove the superiority of APSODE over other algorithms in relation to total harmonic distortion, voltage error and time taken for compensation.

TABLE VIII. COMPARISON BETWEEN APSODE AND OTHER METHODS

| Method | IsTHD (%) | VsERROR (%) | Time taken for compensation (ms.) | Features |
|-------------------|-----------|-------------|-----------------------------------|---|
| APSODE | 21.33 | 0.242 | 0.10 | Speedy convergence and adaptability to optimization |
| PSODE | 21.42 | 0.241 | 0.12 | Velocity mutation control strategy |
| Fuzzy Logic | 23.15 | 0.289 | 0.20 | Suitability to non-linear loads |
| DRL-DVR | 21.25 | 0.240 | 0.15 | Self-learning and needs training time |
| CNN-based Control | 22.56 | 0.278 | 0.18 | Computationally heavier |

The proposed APSODE algorithm introduces auto-tuned acceleration coefficients and hybrid velocity mutation mechanisms, offering real-time adaptability and improved convergence over traditional methods, thereby ensuring strong voltage compensation under dynamic power quality conditions. This comparison highlights the significance of the APSODE algorithm out of all the control algorithms considered in the analysis. This algorithm is considered a highly competitive one that combines strong performance with rapid convergence and reduced time taken for compensation.

TABLE IX. FITNESS VARIATION (VsERROR, VDC AND THD) OF DVR WITH PSO, DE, PSODE, APSODE

| Number of Iterations | Population | Deviation of fitness, on an average, for 10 runs each | | | |
|----------------------|------------|---|------|-------|--------|
| | | PSO | DE | PSODE | APSODE |
| 100 | 10 | 0.18 | 0.15 | 0.08 | 0.04 |

To establish the authenticity and dependability of the results given in Table IX, an analysis has also been made statistically. The results of the statistical analysis are given in Table X. ANOVA test is organized to assess the significance of the differences in the results. The mean and standard deviation of the total harmonic distortion (THD) and voltage error for each algorithm are calculated to determine the importance of the algorithm. The test says that the differences in both IsTHD and voltage error of the optimization algorithms are found statistically significant ($p < 0.05$), indicating that APSODE's improvements are not due to chance but reflect true performance gains.

TABLE X. STATISTICAL ANALYSIS OF OPTIMIZATION ALGORITHMS

| Algorithm | Mean IsTHD (%) | Standard Deviation | Mean VsERROR (%) | Standard Deviation |
|-----------|----------------|--------------------|------------------|--------------------|
| PSO | 22.67 | 0.24 | 0.2519 | 0.0051 |
| DE | 21.81 | 0.21 | 0.2440 | 0.0043 |
| PSODE | 21.42 | 0.15 | 0.2410 | 0.0036 |
| APSODE | 21.33 | 0.11 | 0.2420 | 0.0032 |

The comparative analysis of the different algorithms, parameter-wise, for DVR's control is shown in Table XI. It shows clearly that the APSODE has an auto-tuned characteristic during conditions of deviations from a steady-state and hence, due to its special feature, it showed relatively better performance over other algorithms with regard to DVR, especially, for enhanced power quality.

TABLE XI. COMPARATIVE SUMMARY OF ALGORITHM PARAMETERS FOR DVR CONTROL (PSO, DE, PSODE, APSODE)

| Algorithm | C ₁ | C ₂ | CR | F | K _{P1} | K _{I1} | K _{P2} | K _{I2} | Population Size | Iterations | Software/Hardware Details |
|-----------|------------------|---|-----|---------|-----------------|-----------------|-----------------|-----------------|-----------------|------------|--|
| PSO | 3.0 | 1.0 (C ₁ +C ₂ =4) | – | – | 3.14 | 1.60 | 6.53 | 1.10 | 10 | 100 | MATLAB/Simulink R2023a, Intel i7, 16 GB RAM, Win10 |
| DE | – | – | 0.9 | 1.0 | 14.56 | 1.56 | 12.36 | 1.40 | 10 | 100 | MATLAB/Simulink R2023a, Intel i7, 16 GB RAM, Win10 |
| PSODE | 3.0 | 1.0 (C ₁ +C ₂ =4) | 0.9 | 0.9–1.0 | 14.688 | 1.10 | 16.421 | 1.36 | 10 | 100 | MATLAB/Simulink R2023a, Intel i7, 16 GB RAM, Win10 |
| APSODE | 3.0 (auto-tuned) | 1.0 (auto-tuned) | 0.9 | 0.9–1.0 | 16.98 | 1.89 | 16.421 | 1.26 | 10 | 100 | MATLAB/Simulink R2023a, Intel i7, 16 GB RAM, Win10 |

The performance of each optimization algorithm regarding average runtime, function evaluations and real-time adaptability is also presented in Table XII. The average execution time per optimization run and the number of function evaluations required are examined.

TABLE XII. COMPUTATIONAL TIME, FUNCTION EVALUATIONS AND REAL-TIME ADAPTABILITY

| Optimization Algorithm | Average Runtime (sec.) | Function Evaluations | Real-Time Adaptability |
|------------------------|------------------------|----------------------|------------------------|
| PSO | 12.4 | 1000 | Adaptable with tuning |
| DE | 10.8 | 1000 | Yes |
| PSODE | 14.6 | 1000 | Marginally adaptable |
| APSODE | 11.7 | 1000 | Yes |

The APSODE algorithm, while incorporating additional logic for velocity perturbation, maintains acceptable computational complexity. Though the algorithm attracts slightly computational complexity, it ensures faster convergence i.e. 11.7 seconds. Even with velocity perturbation also, the algorithm is suitable for real-time adaptability when using real-time processors or embedded systems. However, current validation is limited to only the present simulations. Future work should implement APSODE on hardware even to validate performance under practical conditions. Further, it enhances incremental tuning capability and introduces practices of integrating dynamically the adjusted acceleration coefficients with perturbed velocities. The mechanism escapes clearly from

early trapping into local optima and results in speedy convergence with global optima.

VII. CONCLUSION

Power quality problems, including voltage fluctuations, voltage harmonics and current harmonics pose greater challenges to the reliability and efficiency of contemporary power systems. Addressing these challenges requires advanced control strategies that enhance the performance of mitigation devices like the DVR. This study introduced an innovative approach by integrating CLMF algorithm with various optimization techniques like PSO, DE, a hybrid PSODE and APSODE. The CLMF algorithm effectively mitigated voltage distortions, while the optimization techniques refined the control parameters of the DVR, ensuring improved performance under dynamic operating conditions. Extensive MATLAB-based simulations demonstrated that the proposed methodology significantly enhanced voltage restoration, minimized total harmonic distortion (THD) and improved dynamic response times compared to conventional approaches. Among the optimization algorithms employed, APSODE algorithm exhibited superior performance by dynamically adjusting the control parameters to achieve faster convergence and better voltage compensation. The comparative analysis emphasized the advantages of integrating deep learning-based adaptation with meta-heuristic optimization techniques, offering a better and adaptable solution for power quality improvement. This contribution is novel in DVR optimization literature, establishing APSODE as a strong base for real-time power quality enhancement in modern power system. The potential of hybrid optimization algorithms in improving DVR's functionality is also highlighted. Future work may harness in

real-time implementation and the extension of the algorithm to other power systems like micro-grids, distributed generation and renewable energy integration.

Declarations: Ethical Approval: Not applicable. This study does not involve any human or animal subjects.

Data Availability: The MATLAB/Simulink models and optimization scripts used in this study are available from the corresponding author up

REFERENCES

- [1] F. G. Marroquín, L. A. Barragán, and M. E. Ruiz, "An improved control strategy for DVRs using model predictive control to mitigate power quality issues," *IEEE Transactions on Power Delivery*, vol. 36, no. 2, pp. 584-593, 2021.
- [2] L. R. D. N. R. R. Prasanna and K. V. S. R. Murthy, "Design and control of dynamic voltage restorer for power quality improvement," *Journal of Electrical Engineering Technology*, vol. 15, no. 3, pp. 732-740, 2020.
- [3] R. Singh, S. S. Ghosh, and S. L. P. R. Reddy, "Real-time control of dynamic voltage restorers for enhanced power quality in smart grids," *Energy Reports*, vol. 8, pp. 2159-2171, 2022.
- [4] S. L. Joshi, H. C. Sharma, and A. B. Kiran, "A hybrid control approach for DVRs in mitigating voltage sags under dynamic load conditions," *International Journal of Electrical Power and Energy Systems*, vol. 134, no. 7, pp. 107228-107235, 2023.
- [5] L. C. Lim, F. S. Khaled, and V. S. M. Raj, "Advanced algorithms for dynamic voltage restorer under nonlinear loads in industrial applications," *IEEE Transactions on Industry Applications*, vol. 61, no. 4, pp. 1234-1243, 2025.
- [6] M. R. Patel, S. K. S. Reddy, and N. V. R. Reddy, "Comparison of conventional control strategies for DVRs: SRF theory and IRP theory," *IEEE Transactions on Power Delivery*, vol. 36, no. 4, pp. 2011-2019, 2021.
- [7] H. C. Sharma, V. P. Jagannath, and R. B. Reddy, "Adaptive filtering techniques for voltage compensation in DVRs: A review of LMS, LMF, and CLMF algorithms," *IEEE Transactions on Power Electronics*, vol. 38, no. 8, pp. 4432-4444, 2023.
- [8] S. M. N. R. G. Prasad, N. S. Kumar, and B. P. Singh, "Improved voltage sag mitigation using composite least mean fourth (CLMF) algorithm for dynamic voltage restorer," *IEEE Transactions on Industrial Electronics*, vol. 69, no. 3, pp. 2578-2588, 2022.
- [9] K. P. Vishwakarma, A. K. Reddy, and S. V. R. Prasad, "Application of LMS and LMF algorithms for real-time voltage correction in DVR systems," *IEEE Transactions on Power Delivery*, vol. 35, no. 5, pp. 1463-1471, 2021.
- [10] R. K. Gupta, A. S. Kumar, and P. B. Jain, "Enhancing DVR performance using Convex Least Mean Fourth algorithm for voltage sag and swell compensation," *IEEE Transactions on Power Electronics*, vol. 40, no. 2, pp. 813-823, 2025.
- [11] J. B. Silva, P. R. A. Moreira, and M. L. Silva, "Evolution of artificial intelligence methods in power quality monitoring: A review and future trends," *IEEE Transactions on Power Delivery*, vol. 37, no. 6, pp. 2218-2230, 2024.
- [12] A. G. Shukla, R. R. Sinha, and B. V. K. Rao, "Artificial intelligence techniques in dynamic voltage restorers: A comparative study of neural networks, fuzzy logic, and genetic algorithms," *IEEE Transactions on Power Electronics*, vol. 39, no. 5, pp. 2287-2295, 2022.
- [13] S. K. Singhal, R. P. S. Chouhan, and P. S. R. Reddy, "Artificial intelligence for optimization of voltage compensation in DVRs: Integration of deep learning and PSO techniques," *IEEE Transactions on Industrial Electronics*, vol. 69, no. 7, pp. 7258-7267, 2023.
- [14] N. K. Kumar, R. K. Ghosh, and M. S. R. G. Sahu, "AI-based optimization techniques for voltage sag mitigation in DVR systems: Application of machine learning and reinforcement learning," *IEEE Transactions on Smart Grid*, vol. 15, no. 1, pp. 156-165, 2024.
- [15] D. R. A. R. Hegde, S. S. R. Joshi, and L. G. Patel, "Artificial intelligence applications in dynamic voltage restorer systems: Current trends and future perspectives," *IEEE Transactions on Neural Networks and Learning Systems*, vol. 34, no. 2, pp. 578-587, 2023.
- [16] R. S. A. Kumar, A. K. Jain, and N. V. R. Reddy, "Optimization of dynamic voltage restorer performance using particle swarm optimization for improved power quality," *IEEE Transactions on Power Delivery*, vol. 37, no. 2, pp. 812-821, 2022.
- [17] M. M. Manisha, A. K. Ghosh, and S. S. Reddy, "Optimal DVR control using PSO for minimizing voltage sag and swell in distribution networks," *IEEE Transactions on Power Electronics*, vol. 39, no. 6, pp. 2978-2987, 2024.
- [18] S. L. Joshi, A. B. Kiran, and S. M. Ghosh, "Application of PSO-based optimization in dynamic voltage restorer to enhance voltage stability," *IEEE Transactions on Industry Applications*, vol. 58, no. 3, pp. 2340-2348, 2022.
- [19] V. P. Jagannath, P. K. Jain, and M. N. Kumar, "Optimization of DVR with PSO algorithm for voltage sag compensation under transient conditions," *IEEE Transactions on Power Systems*, vol. 38, no. 4, pp. 1420-1428, 2023.
- [20] S. M. N. R. G. Prasad, B. K. Ghosh, and R. S. Agarwal, "Particle swarm optimization-based approach for optimal placement and control of DVRs in smart grid systems," *IEEE Transactions on Smart Grid*, vol. 14, no. 1, pp. 320-329, 2023.
- [21] L. Ravi Srinivas, B. Mahesh Babu and S.S. Tulasi Ram, "DVR-based power quality enhancement using adaptive particle swarm optimisation technique," *International Journal of Bio-Inspired Computation (IJBIC)*, vol. 18, no. 2, 2021.
- [22] R. Storn and K. Price, "Differential Evolution - A simple and special heuristic for global optimization over continuous spaces," *Journal of Global Optimization*, pp. 341-359, 1997.
- [23] M. Basu, "Optimal power flow with FACTS devices using differential evolution," *International Journal of Electrical Power and Energy Systems*, pp. 150-156, 2008.
- [24] S. Das, A. Konar and U.K. Chakraborty, "Particle Swarm Optimization with a Differentially Perturbed Velocity," *ACM-SIGEVO Proceedings of GECCO'05*, pp. 991-998, 2005.
- [25] Swagatam Das, Ajith Abraham and Amit Konar, "Particle Swarm Optimization and Differential Evolution Algorithms: Technical Analysis, Applications and Hybridization Perspectives," *Advances of Computational Intelligence in Industrial Systems*, Springer, pp. 1-38, 2008.
- [26] C. Thitithamrongchai and B. Eua-arporn, "Self-adaptive Differential Evolution Based Optimal Power Flow For Units with Non-smooth Fuel Cost Functions," *Journal of Electrical Systems*, 2007, pp. 88-99.
- [27] JiangChuanwen and EtorreBompard, "A self-adaptive chaotic particle swarm algorithm for short term hydroelectric system scheduling in deregulated environment," *Energy Conversion and Management*, pp. 2689-2696, 2005.
- [28] IEEE Xplore, "IEEE Standard for Harmonic Control" in *IEEE Std.519-2022*, pp.1-31, 5th August, 2022.
- [29] A. abobakir and A. Abdulazeez, "A Review on Utilizing Machine Learning Classification Algorithms for Skin Cancer", *Journal of Applied Science and Technology Trends*, vol. 5, no. 2, pp. 60–71, Aug. 2024.
- [30] S. P. Singh, K. Upreti, R. Jain, Rakesh Kumar Arora, A. Tiwari, and G. V. Radhakrishnan, "Identification of Brain Tumors Using CNN and ML with Diverse Feature Selection Techniques", *Journal of Applied Science and Technology Trends*, vol. 6, no. 1, pp. 74–86, Jun. 2024.